Electronic Supplementary Material (ESI) for Sustainable Energy & Fuels.


Supplementary Information for

# Disordered Surface Formation of $WS_2$ via Hydrogen Plasma with Enhanced Anode Performances for Lithium and Sodium Ion Batteries

Hongmei Wang [a], Qian Yuan [a], Dong Wang*[a], Ge Chen*[b], Xing Cheng [b], Thomas Kups [a] and Peter Schaaf [a]

a FG Werkstoffe der Elektrotechnik, Institut für Werkstofftechnik und Institut für Mikro- und Nanotechnologien MacroNano®, TU Ilmenau, Gustav-Kirchhoff-Str. 5, 98693 Ilmenau, Germany

b Beijing Key Laboratory for Green Catalysis and Separation, College of Environmental & Energy Engineering, Beijing University of Technology, Pingleyuan 100, 100124 Beijing, P. R. China.

*E-mail: dong.wang@tu-ilmenau.de ; chenge@bjut.edu.cn

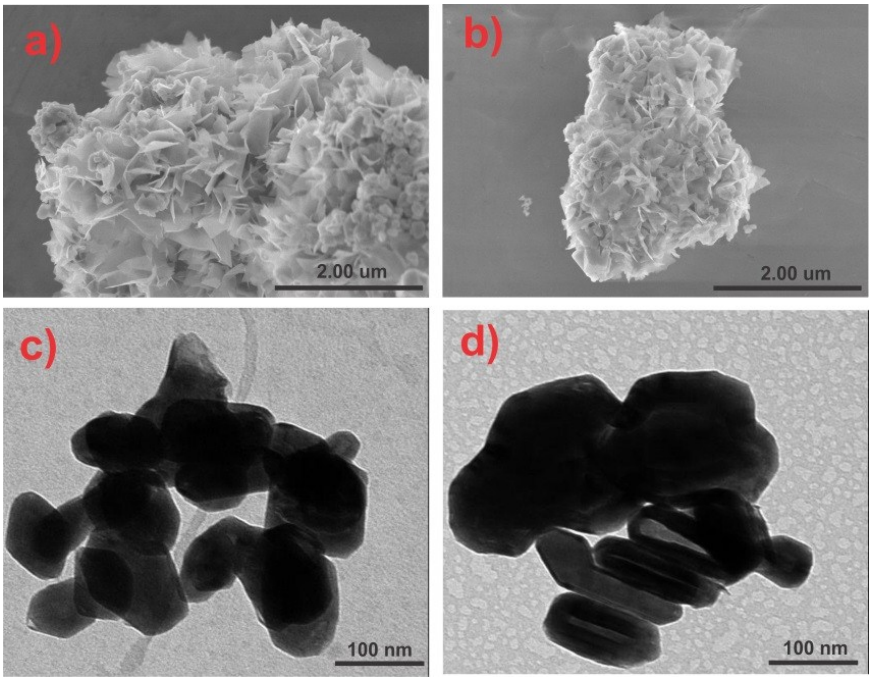


Figure S1. (a) (c) SEM and TEM images of pristine $WS_2$; (b)(d) SEM and TEM images of hydrogenated $WS_2$.

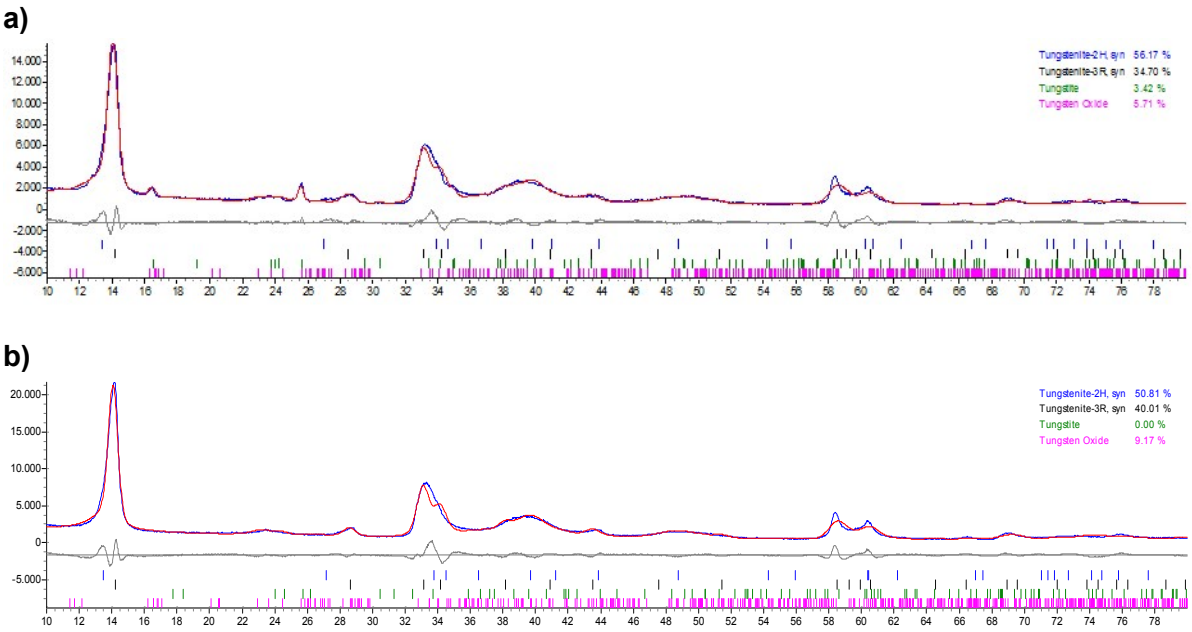


Figure S2. Full pattern quantitative analysis in TOPAS. (a) Pristine $WS_2$ nanoparticles, (b) hydrogenated $WS_2$ nanoparticles.

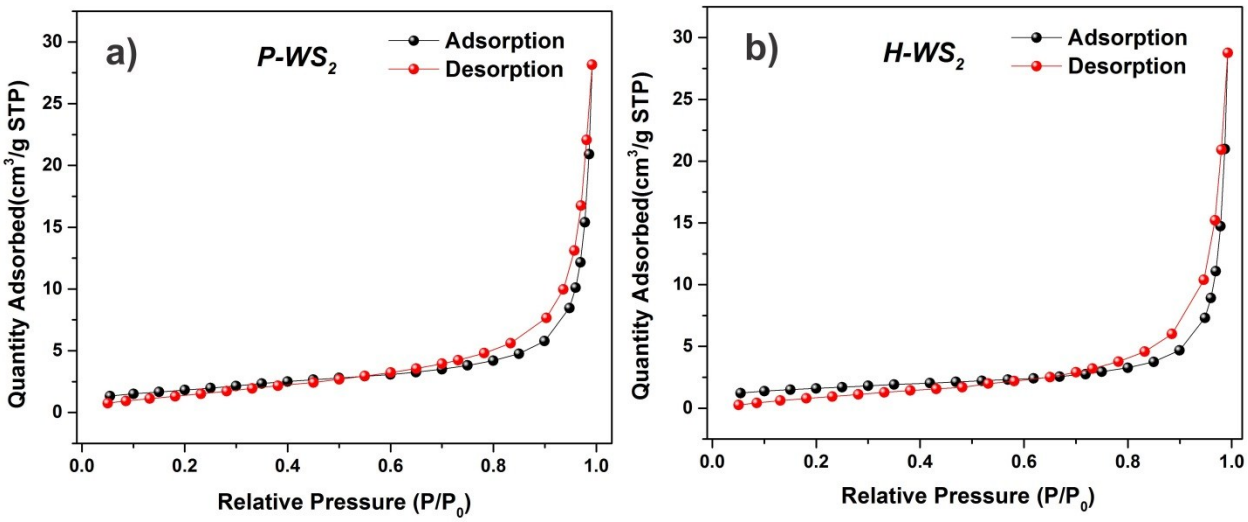


Figure S3. (a) $N_2$ adsorption/desorption isotherms of pristine $WS_2$; (b) $N_2$ adsorption/ desorption isotherms of H-$WS_2$.

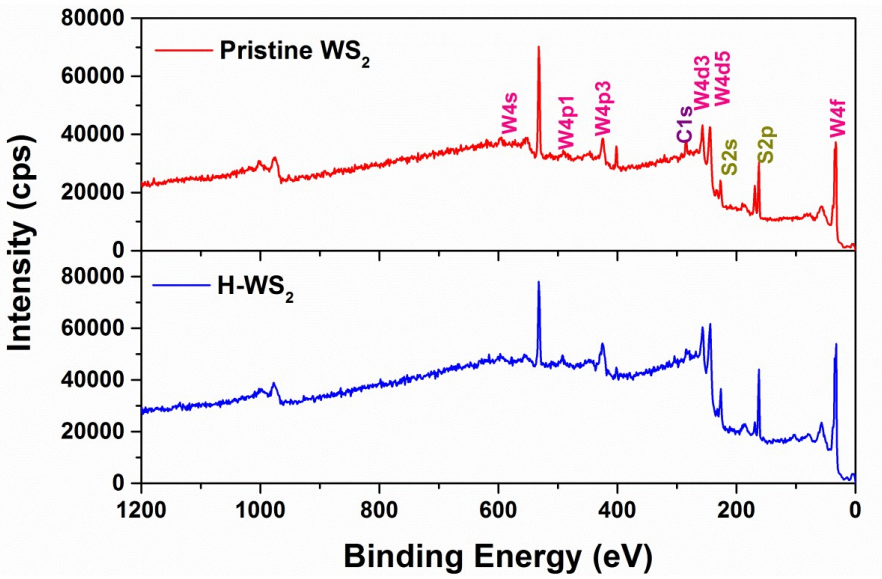


Figure S4. XPS survey spectra of the pristine and hydrogenated $WS_2$ nanoparticles.

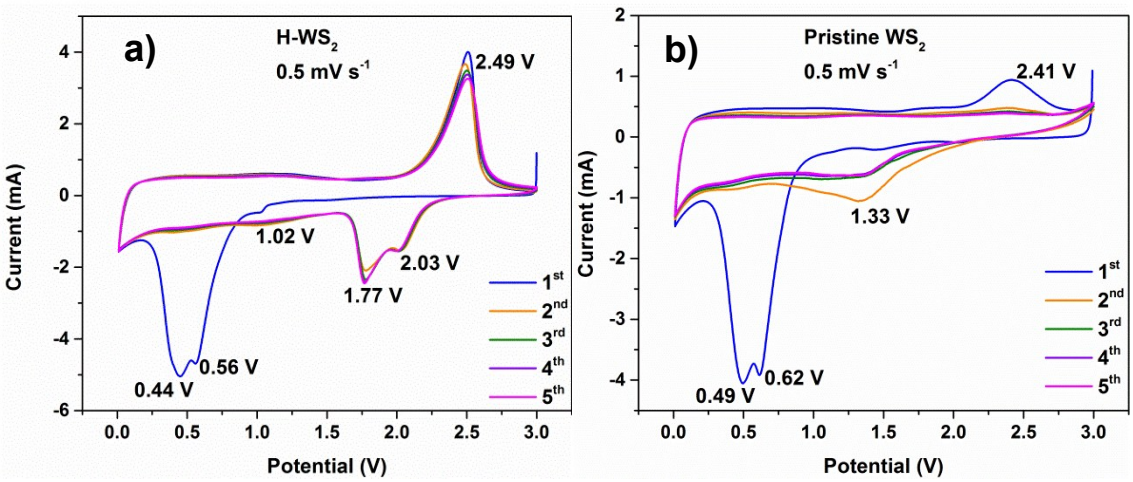


Figure S5. CVs for the (a) H-$WS_2$ and (b) pristine $WS_2$ electrodes measured at a scan rate of 0.5 mV·$s^{-1}$ for different cycles of lithium ion batteries.

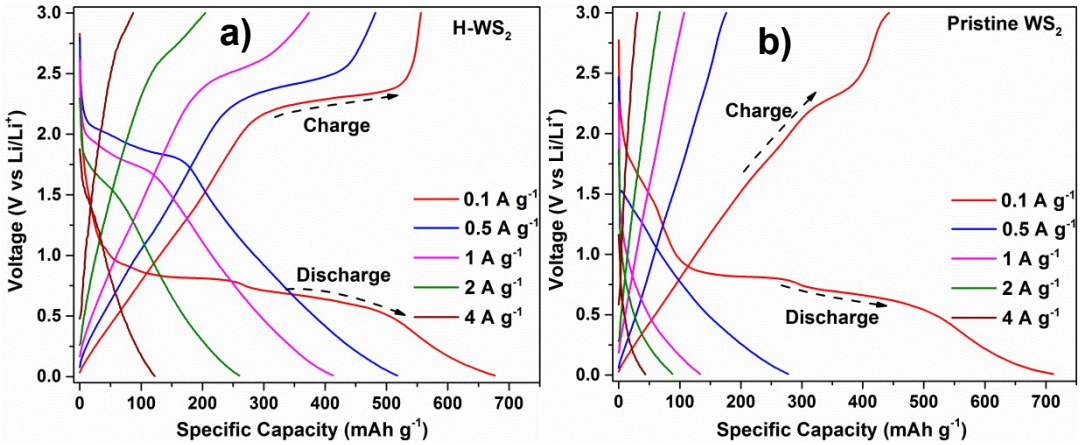


Figure S6 (a) Initial discharge/charge curves of H-$WS_2$ at different rate in the potential window of 0.01–3.0 V, (b) Initial discharge/charge curves of pristine $WS_2$ at different rate in the potential window of 0.01–3.0 V of lithium ion batteries.

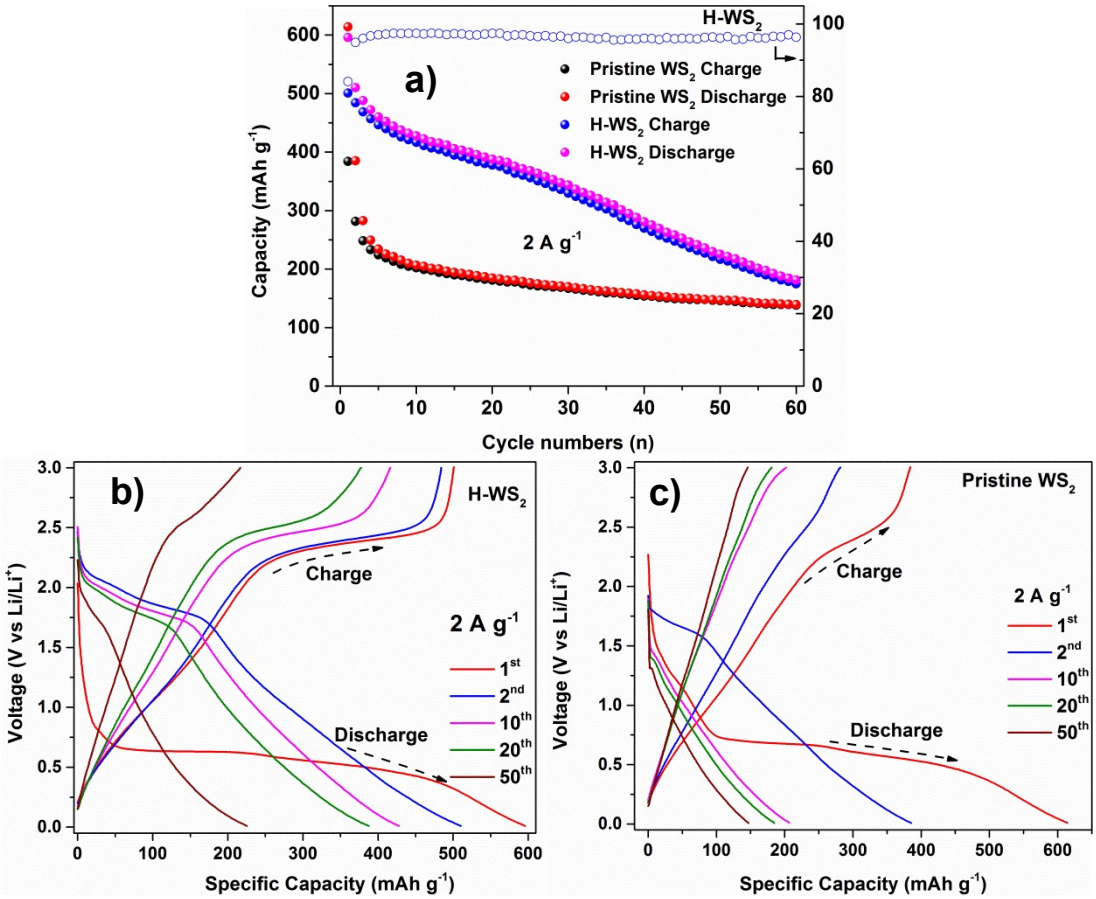


Figure S7. (a) Long term performances and the coulombic efficiencies of samples at charging/discharging rate of 2.0 A·$g^{-1}$ for 60 cycles, (b) Initial discharge/charge curves of H-$WS_2$ at 2.0 A·$g^{-1}$ for different cycles in the potential window of 0.01-3.0 V, (c) Initial discharge/charge curves of pristine $WS_2$ at 2.0 A·$g^{-1}$ for different cycles in the potential window of 0.01–3.0 V of lithium ion batteries.

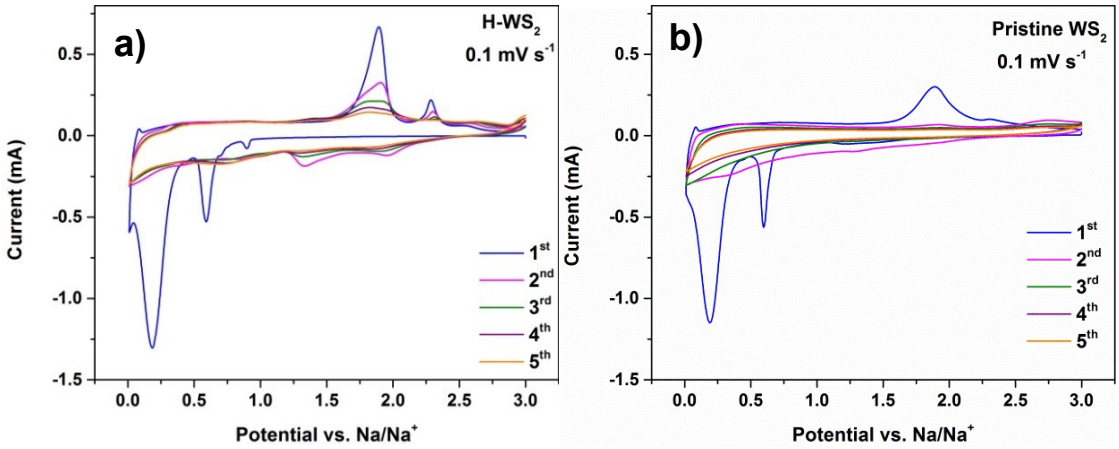


Figure S8. CVs for the (a) H-$WS_2$ and (b) pristine $WS_2$ electrodes measured at a scan rate of 0.1 mV·$s^{-1}$ for different cycles of sodium ion batteries.

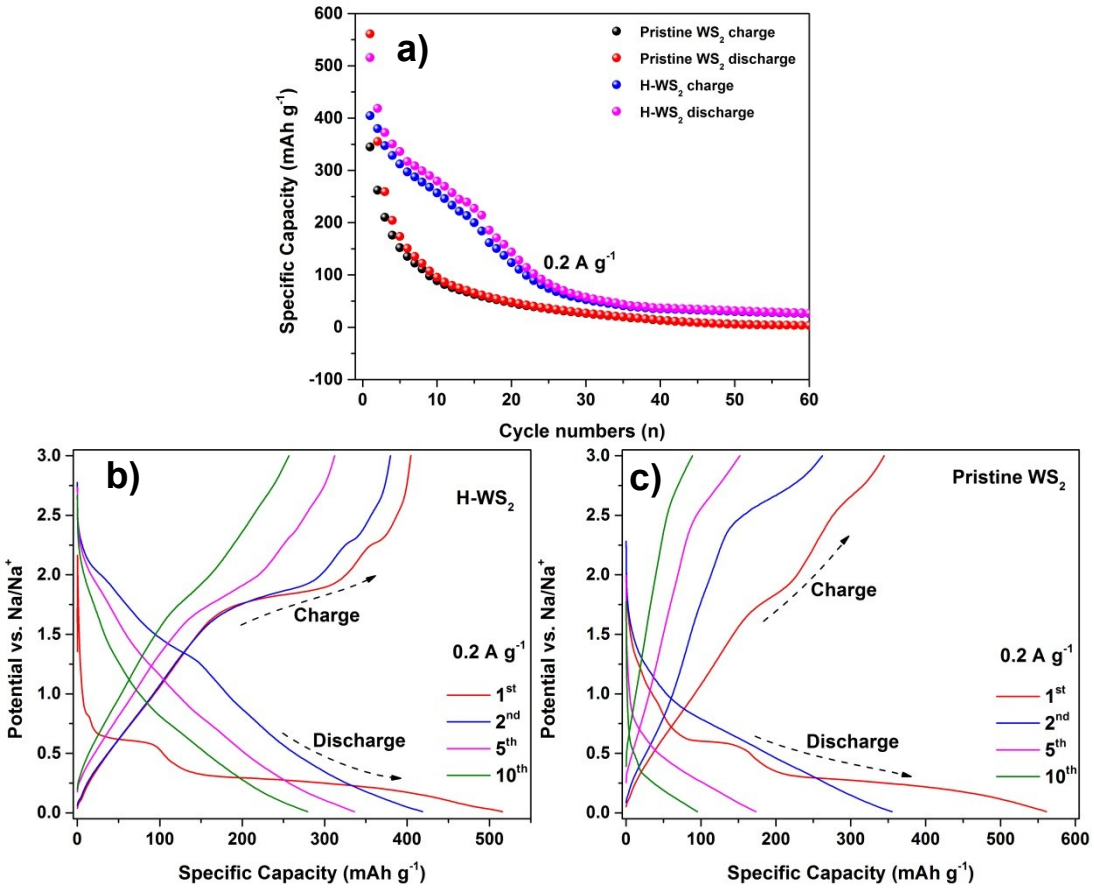


Figure S9. (a) Long term performances of samples at charging/discharging rate of 0.2 A·$g^{-1}$ for 60 cycles, (b) Initial discharge/charge curves of H-$WS_2$ at 0.2 A·$g^{-1}$ for different cycles in the potential window of 0.01-3.0 V, (c) Initial discharge/charge curves of pristine $WS_2$ at 0.2 A·$g^{-1}$ for different cycles in the potential window of 0.01–3.0 V of sodium ion batteries.

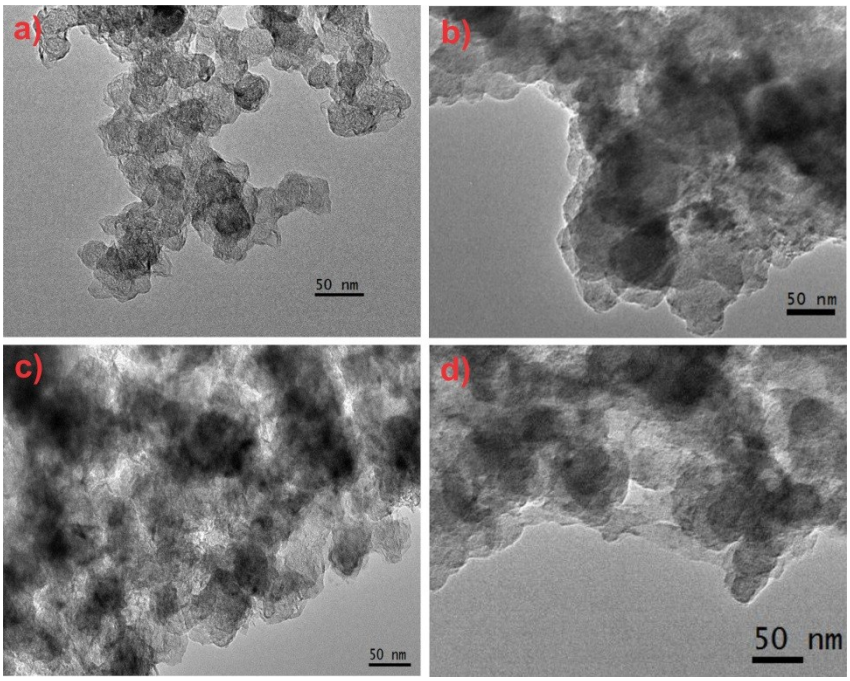


Figure S10. TEM images of (a) pristine $WS_2$, (b) H-$WS_2$ after rate performance testing of lithium ion batteries; TEM images of (c) pristine $WS_2$, (d) H-$WS_2$ after rate performance testing of sodium ion batteries.

Table S1. Phase wt % of pristine and hydrogenated $WS_2$ nanoparticles.

| Phases | Tungstenite 2H | Tungstenite 3R | Tungstite | Triclinic $WO_3$ |
|---|---|---|---|---|
| Pristine $WS_2$ | 56.17% | 34.70% | 3.42% | 5.71% |
| H-$WS_2$ | 50.81% | 40.01% | 0% | 9.17% |

Table S2. Fitted impedance parameters for the electrodes of (a) LIBs and (b) SIBs.

a) LIBs

| Electrode | $R_S$ (Ω) | $R_{SEI}$ (Ω) | $R_C$ (Ω) |
|---|---|---|---|
| Pristine $WS_2$ | 2.93 | 132.4 | 313.5 |
| H-$WS_2$ | 3.47 | 3.817 | 7.173 |

b) SIBs

| Electrode | $R_S$ (Ω) | $R_{SEI}$ (Ω) | $R_C$ (Ω) |
|---|---|---|---|
| Pristine $WS_2$ | 7.766 | 433.2 | 1177 |
| H-$WS_2$ | 4.933 | 117.6 | 260.5 |

Table S3 Comparison of $WS_2$ anode material for batteries between current work and related references.

| Active material | Discharge capacity (mAh/g) | Current density (mA/g) | Cycle numbers | Battery type | Ref. |
|---|---|---|---|---|---|
| H-$WS_2$ | 596/515 | 2000 | 60 | LIBs / SIBs | Current work |
| Sulfuration $WS_2$ | ~800 | 800 | 50 | LIBs | 17 |
| Ordered mesoporous $WS_2$ | ~700 | 100 | 100 | LIBs | 31 |
| Surface functionalized $WS_2$ sheets | 465 | 25 | 50 | LIBs | 62 |
| $WS_2$ nanowires | 605.3 | 100 | 50 | SIBs | 70 |
| 3D porous $WS_2$/C | 267 | 500 | 300 | SIBs | 71 |
| $WS_2$-NC | 450 | 1000 | 100 | SIBs | 72 |
| $WS_2$ composite | 519 | 100 | 100. | LIBs | 73 |
| Few-layer $WS_2$ | 45 | 1000 | 50 | LIBs | 74 |
| $WS_2$ @NGr | 455/289 | 1000 | 140/60 | LIBs / SIBs | 75 |
| Graphene-like $WS_2$ nanosheets | 550 | 43.2 | 70 | LIBs | 76 |
| $WS_2$ nanosheets @carbon | 512/616 | 200 | 100/100 | LIBs / SIBs | 77 |
| Porous $WS_2$ in CMK-3 matrix | 720/450 | 100 | 100/70 | LIBs / SIBs | 78 |